Experimental and Numerical Examination of the Thermal Transmittance of High Performance Window Frames

Arild Gustavsen, PhD *Member ASHRAE*
Howdy Goudey
Dariush Arasteh, PE *Member ASHRAE*
Sivert Uvsløkk
Goce Talev
Bjørn Petter Jelle, PhD
Christian Kohler *Member ASHRAE*

ABSTRACT

While window frames typically represent 20%–30% of the overall window area, their impact on the total window heat transfer rates may be much larger. This effect is even greater in low-conductance (highly insulating) windows that incorporate very low conductance glazings. Developing low-conductance window frames requires accurate simulation tools for product research and development.

The Passivhaus Institute in Germany states that windows (glazing and frames, combined) should have U-factors not exceeding 0.80 W/(m^2·K). This has created a niche market for highly insulating frames, with frame U-factors typically around 0.7-1.0 W/(m^2·K). The U-factors reported are often based on numerical simulations according to international simulation standards. It is prudent to check the accuracy of these calculation standards, especially for high-performance products, before more manufacturers begin to use them to improve other product offerings.

In this paper, the thermal transmittance of five highly insulating window frames (three wooden frames, one aluminum frame, and one polyvinyl chloride frame), found from numerical simulations and experiments, are compared. Hot box calorimeter results are compared with numerical simulations according to ISO 10077-2 and ISO 15099 (ISO 2003a, 2003b). In addition, computational fluid dynamics simulations were carried out in order to use the most accurate tool available to investigate the convection and radiation effects inside the frame cavities.

Our results show that available tools commonly used to evaluate window performance, based on ISO standards, give good overall agreement, but specific areas need improvement.

INTRODUCTION

Energy use in buildings accounts for a significant part of energy use and greenhouse gas emissions. New building regulations and new measures have been introduced to improve the energy efficiency of buildings. One of these measures is improved windows with a low thermal transmittance (U-factor). Still, windows use typically 25% of the heating and cooling energy in buildings. Energy-efficient retrofits and zero-energy buildings will require windows that insulate better than today's best windows. Such products will also increase comfort and allow the use of more efficient and smaller HVAC systems and air distribution or hydronic systems.

Today, the best windows have a U-factor of about 0.8 W/(m^2·K). These windows are often called *passive-house windows*, as windows with a thermal transmittance less than or equal to 0.8 W/(m^2·K) can be certified by the Passivhaus Institute in Germany (Passiv 2010). In order for the thermal transmittance of a window to be found, numerical simulations or experiments are needed, in accordance with various international standards. EN ISO 12567-1 (CEN 2000) is usually followed for hot box calorimeter experiments. Numerical simulations are usually carried out according to either ISO 15099 or ISO 10077-2 (ISO 2003b, 2003a), where ISO 15099 usually is considered to be the most accurate (it also bases its models on cited references).

Arild Gustavsen *is a professor in the Department of Architectural Design, History and Technology, Norwegian University of Science and Technology (NTNU), Norway.* ***Howdy Goudey*** *is a researcher,* ***Dariush Arasteh*** *is deputy group leader, and* ***Christian Kohler*** *is a researcher in the Windows and Daylighting Group, Lawrence Berkeley National Laboratory, CA, USA.* ***Sivert Uvsløkk*** *is a senior research scientist in the Department of Materials and Structures, SINTEF Building and Infrastructure, Norway.* ***Bjørn Petter Jelle*** *is a senior research scientist in the Department of Materials and Structures, SINTEF Building and Infrastructure, Norway, and an associate professor in Department of Civil and Transport Engineering, NTNU, Norway.* ***Goce Talev*** *is a research fellow in the Department of Civil and Transport Engineering, NTNU, Norway.*

These standards differ with respect to both air cavity modeling and boundary condition treatment. In addition to the standards, there are also organizations that specify additional (and usually more detailed rules) for how the thermal transmittance should be found—the National Fenestration Rating Council (NFRC), for example, whose procedures may be found in the *THERM 5.2/WINDOW 5.2 NFRC Simulation Manual* (Mitchell et al. 2006). Still, questions are often raised regarding the accuracy of the various calculation procedures (Gustavsen et al. 2008) and especially regarding their usability for high-performance window frames such as passive-house windows.

In this paper the thermal transmittance of five high-performance window frames are studied in detail (one thermally broken aluminum frame, two thermally broken wooden frames, one partially thermally broken wooden frame, and one multi-cellular polyvinyl chloride [PVC] frame). Hot box results are compared with numerical simulations according to ISO 10077-2 and ISO 15099 (ISO 2003a, 2003b). In addition, computational fluid dynamics (CFD) simulations were carried out to further investigate the effect of the convection and radiation effects inside the frame cavities.

WINDOW FRAMES

Five different frames were selected: one thermally broken aluminum frame (Frame A), two thermally broken wooden frames (Frames B and C), one partially thermally broken wooden frame (Frame D), and one frame made of PVC (Frame E). The two thermally broken wooden frames (Frames B and C) had a thermal break of polyurethane in the middle of the sill, jambs, and head. The partially thermally broken wooden frame (Frame D) had a thermal break in only the jambs and the head. All the frames were of the inward opening casement type. The windows were chosen to include the effects that may complicate typical computer simulations of thermal performance using ISO standards: cladding, thermal bridging, use of multiple materials, convection and radiation in hollow cavities, and operating hardware.

Frames A, B, and C were tested both with a glazing and with an expanded polystyrene (EPS) foam board (instead of glazing) in the hot box. Frame D was tested with a double glazing and Frame E was tested with an insulation panel. Frame materials and frame sizes are shown in Table 1. Total window sizes and thicknesses of EPS insulation panels are shown in Table 2. The window sizes were selected due to the dimensions of the hot box at SINTEF Building and Infrastructure in Trondheim. The frames are further described in the following sections, with figures showing the geometry and insulating elements.

Table 1. Frame Materials and Sill, Jamb, and Head Sizes

Frame	Structural Material	Insulation Material	Sill/Jamb/Head Heights, mm
A	Aluminum	Polyurethane	110 / 110 / 110
B	Wood	Polyurethane	138 / 119 / 119
C	Wood	Polyurethane	101 / 94 / 105
D	Wood	Polyurethane	101 / 94 / 105
E	PVC	Polyurethane	117 / 117 / 117

Table 2. Total Size of Window Samples Tested in Hot Box, as Well as the Thickness of the Glazing and EPS Insulation Panel

Frame	Height, m	Width, m	Thickness of Insulation Panel, mm
A	1.19	1.19	36
B	1.19	1.19	44
C	1.19	1.19	44
D	1.19	1.19	24
E	1.19	1.19	36

Frame A (Foam-Broken Aluminum)

Frame A is an aluminum frame where the thermal breaks are placed between frame and sash elements (see Figure 1). A thin layer of aluminum cladding is strategically designed to minimize direct connections between inside and outside, over polyurethane solid elements. The frame U_f-factor is reported

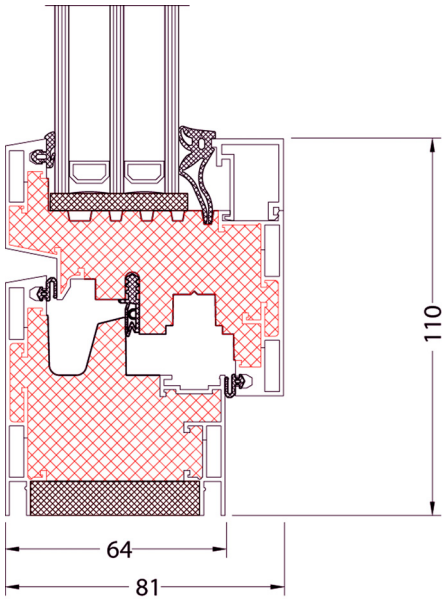

Figure 1 *Cross section of Frame A. The frame has the same cross section for sill, jambs, and head. The steel arrangements for opening and closing the window are not shown in the figure but are taken into account in the simulations. The units in the figure are mm.*

to be 1.0 W/(m^2·K) (a measured value according to EN 12412-2 [CEN 2003]), provided by the manufacturer.

Frame B (Foam-Broken Wood)

Figure 2 shows the various cross-sections for Frame B, which is a frame with thermal breaks of polyurethane between wood in frame and sash elements. The thermal short-circuits from hardware have been minimized. The frame U_f-factor is reported to be 0.73 W/(m^2·K), according to the producer.

Frame C (Foam-broken Wood)

Window frame C is also a thermally broken wood frame (see Figure 3). Polyurethane is used as the thermal break material. According to the producer, the total window U_w-factor is 0.7 W/(m^2·K) with a three-layer glazing (it should be noted that the window U_w-factor generally depends on window size). U_f is not stated. The thermal short-circuits from hardware have been minimized.

Frame D (Foam Partially Broken Wood)

Frame D is similar to Frame C except for the missing thermal breaks in parts of the frame/sash (see Figure 4). The thermal short-circuits from hardware have been minimized. The window U_w-factor is 0.9–1.2 W/(m^2·K) according to the producer. The U_f-factor is not stated.

Frame E (Multi-Cellular PVC)

Window frame E is a PVC window with strategically placed air cavities. Some of the cavities are filled with foam. The frame/sash profile area has been minimized. In addition,

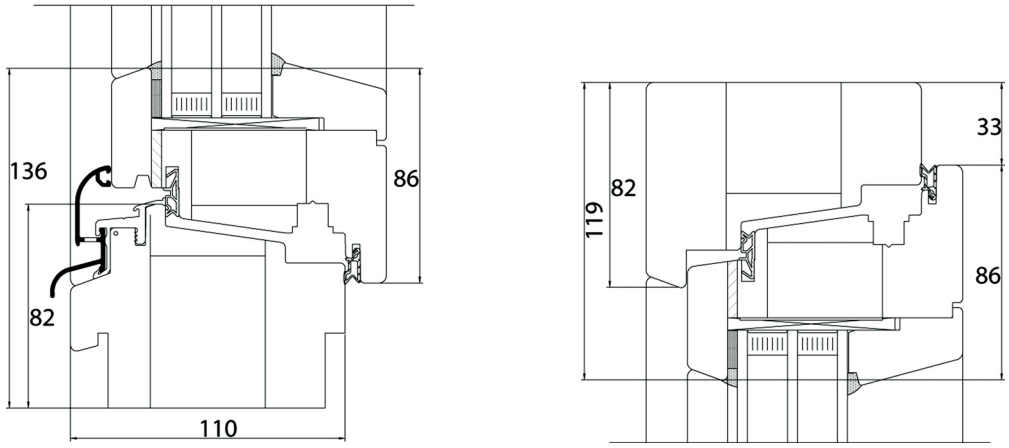

Figure 2 *Cross sections of Frame B. This is a wood frame with polyurethane thermal break. The left figure shows the sill while the right figure shows the head and jambs cross-section. The steel arrangements for opening and closing the window are not shown in the figure, but are taken into account in the simulations. The units in the figure are mm.*

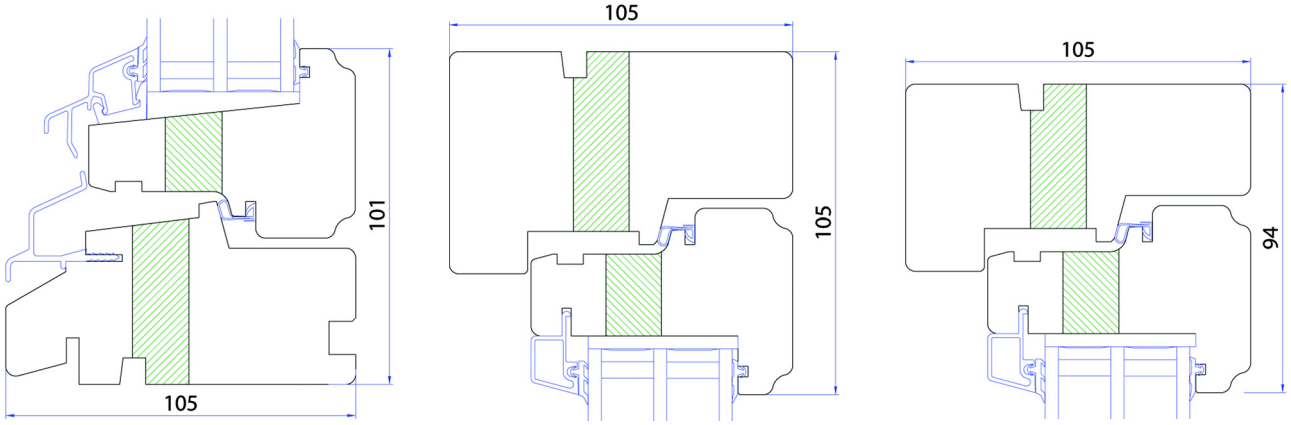

Figure 3 *Cross sections of Frame C. The left image shows the sill cross section, the middle image shows the head, and the right image shows the jamb. The hardware for opening the window is minimized and not continuous throughout the frame section and is not modelled. The units in the figure are mm.*

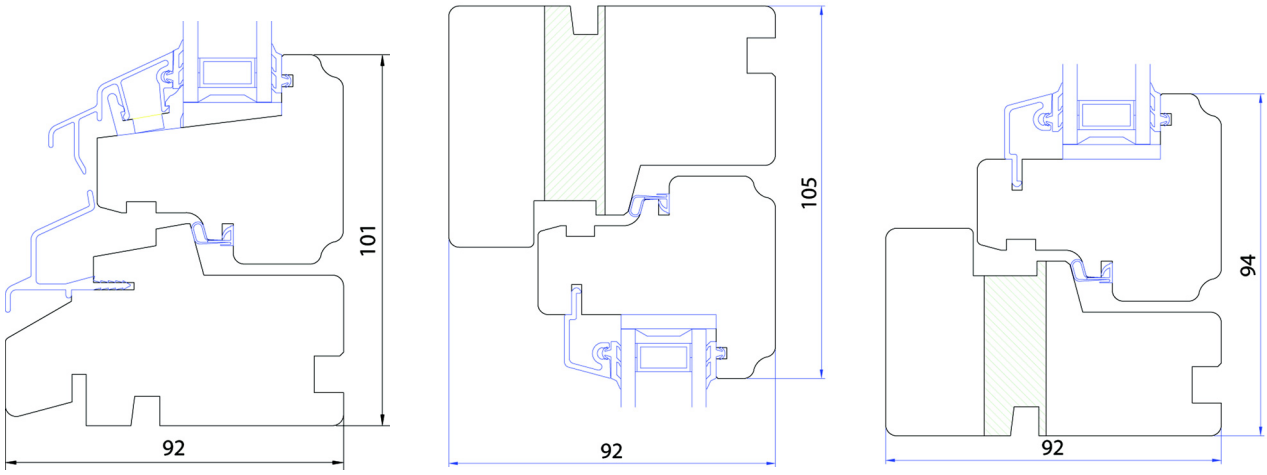

Figure 4 *Cross sections of the partly insulated wooden Frame D. The sill is shown in the left image, the head cross-section is displayed in middle image, and the jamb is shown in the right image. The hardware for opening the window is minimized and not continuous throughout the frame section; it is therefore not modelled. The units in the figure are mm.*

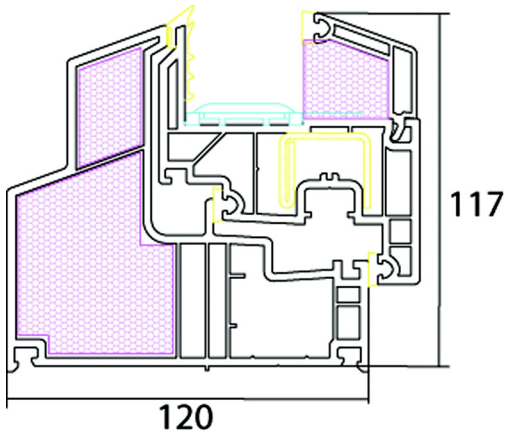

Figure 5 *Cross section of Frame E. The sill, jambs, and head have the same cross-section. The steel arrangements for opening and closing the window are not shown in the figure but are taken into account in the simulations. The units in the figure are mm.*

Figure 6 *Hot box. The cold chamber is to the right and the warm chamber is to the left. The metering area of the hot box is 2.45 × 2.45 m.*

the thermal short-circuits from hardware have been reduced. According to the frame producer, the frame U_f-factor is 0.71 W/(m^2·K).

EXPERIMENTAL PROCEDURE

The measurements were carried out according to EN ISO 12567-1 (CEN 2000), which is an international standard for determining the thermal transmittance (U-factor) of windows and doors by use of a hot box calorimeter. The external view of the guarded hot box is shown in Figure 6. Figure 7 displays the external view of one of the windows as mounted in the hot box.

The windows, which were tested both with an insulation panel and/or a glazing, were mounted into a surround panel of 100 mm EPS and plywood (see Figure 7). The metering area of the hot box is 2.45 × 2.45 m, and the window is placed in a normal position in a wall at a distance of 1.0 m from the floor to the lower edge of the frame. The tests were performed at steady-state conditions at temperatures of +20°C and 0°C at the indoor and outdoor sides, respectively. U-factors at the center of the glazing units were measured by use of a 1 mm thick heat flow meter fixed to the warm side of the glazing unit. Surface temperatures along the vertical centerlines on both sides of the glazing unit were measured by use of thermocouples.

Figure 7 *View of Frame A with glazing mounted in the hot box. The window is seen through an open door (which is closed during measurements) in the baffle panel on the cold (outdoor) side of the hot box. Thermocouples are used to monitor air and surface temperatures for the specimens.*

In the metering box there was natural convection. In the cold box there was forced convection between the window and the baffle by use of fans. The upward airflow parallel to the surface of the specimens was adjusted according to EN ISO 12567-1 procedures (CEN 2000), giving a total average surface resistance ($R_{si} + R_{se}$) of 0.17 (m^2·K)/W.

NUMERICAL PROCEDURE

The numerical simulations were performed with a finite-element method (FEM) simulation program (Finlayson et al. 1998) and a CFD program (Fluent 2005). The FEM tool solves the differential equations in two dimensions, while the CFD program can solve the equations in both two and three dimensions. Both programs are further described in the following sections.

Simulations with the FEM Tool

A FEM program was used to solve the conductive heat-transfer equation. The quadrilateral mesh is automatically generated. Refinement was performed in accordance with Section 6.3.2b of ISO 15099 (ISO 2003b). The energy error norm was less than 6% in all cases, which has been shown to correlate to an error of less than 1% in the total thermal transmittance of typical windows. More information on the thermal simulation program algorithms can be found in Appendix C of Finlayson et al. (1998). The FEM program uses correlations to model convective heat transfer in air cavities, and view factors or fixed radiation coefficients can be used to calculate radiation heat transfer. The convection and radiation coefficients for the frame cavities were calculated according to ISO 15099 (these procedures are also reported in Gustavsen et al. [2005]) and procedures prescribed by Mitchell et al. (2006).

Surface temperatures of cavity walls are among the parameters used to find the equivalent conductivity for frame cavities. At the start of a numerical simulation, these temperatures are set to predefined values that do not necessarily reflect the final temperature distribution of the simulated frame. To find the correct equivalent conductivity for each cavity, cavity wall temperatures have to be adjusted during the calculation. In the FEM program, this adjustment is made automatically, and the temperature tolerance is 1°C (this value is the same in ISO 15099). Thus, when two successive iterations produce temperatures within 1°C of the previous run for all cavity walls, the criterion is satisfied. (In the CFD program, the air cavity wall temperatures also are found as a part of the solution process.)

CFD Simulations

In the CFD program (Fluent 2005), a control-volume method is used to solve the coupled heat and fluid-flow equations in two and three dimensions. Conduction, convection, and radiation are simulated numerically. GAMBIT 2.3.16 (Fluent 2006a) was used as a pre-processor to create the window frame model and to construct the computational domain.

The head and the sill cross-sections were simulated in two dimensions, while the jambs were simulated in three dimensions. Three dimensions are necessary for the jambs because of the three-dimensional nature of the flow for such frame members.

The maximum Rayleigh number found for the frame cavities is about 2×10^4. For the two-dimensional frame members (head and sill sections), the frame cavities have vertical-to-horizontal (L_v/L_h) aspect ratios lower than about six. For such Rayleigh numbers and aspect ratios, Zhao (1998) reports steady laminar flow. For the three-dimensional jamb sections the vertical-to-horizontal aspect ratio might be much larger (L_v/L_h of about 40–100). For two-dimensional cavities with such aspect ratios, both multi-cellular and turbulent flow might occur. However, for three-dimensional cavities with a high vertical-to-horizontal and a low horizontal-horizontal aspect ratio (W/L_h of about 1 [see Figure 11]), Gustavsen and Thue (2007) indicate that laminar flow occurs for some rectangular geometries similar to the ones found in vertical window frames. Although most of the cavities presented are not rectangular, incompressible and steady laminar flow is assumed. Further, viscous dissipation is not addressed, and all thermophysical properties are assumed to be constant except for the buoyancy term of the y-momentum equation where the Boussinesq approximation is used. The Semi-Implicit Method for Pressure-linked Equations Consistent (SIMPLEC) (Van Doormaal and Raithby 1984) was used to model the interaction between pressure and velocity. The energy and momentum variables at cell faces were found by using the Quadratic Upstream Interpolation for Convective Kinetics (QUICK) scheme (Leonard 1979). In addition, the

CFD program uses central differences to approximate diffusion terms and relies on the Pressure Staggering Option (PRESTO) scheme (Fluent 2006b) to find the pressure values at the cell faces. PRESTO is similar to the staggered grid approach described by Patankar (1980). Convergence was determined by checking the scaled residuals and ensuring that they were less than 10^{-7} for all variables.

Radiation heat transfer was included in the simulations through use of the Discrete Transfer Radiation Model (DTRM), which relies on a ray-tracing technique to calculate surface-to-surface radiation (Yao and Fan 1994). The internal cavity walls were assumed to be diffuse gray, and air did not interact with the radiative process.

Prior to the final simulations, some grid sensitivity tests were performed on the sill section of Frame E (the PVC frame). Grid sizes of 0.5, 1, and 2 mm were tested. The frame U-factors only change by 0.3% from the finest to the coarsest mesh. Because it was determined that this difference in grid size was not significant, we used a grid size less than or equal to 2 mm in the final simulations for all of the frames. For the three-dimensional cases (the jambs), a mesh size of 1 cm was used in the vertical direction.

The effect of increasing the number of rays in the radiation heat-transfer algorithm of the CFD code was also tested. Doubling the number of rays resulted in only a 0.1% change in the frame U-factor.

U-Factor Calculation

As noted previously, the windows were measured with both an insulation panel and a glazing (except for Frame D, which was measured with a glazing, and Frame E, which was measured with an insulation panel). In the simulations, however, only windows with insulation panels were modeled.

The frame U-factors, U_f, were calculated from the following equation, as prescribed in ISO 15099 and ISO 10077-2 (ISO 2003b, 2003a):

$$U_f = \frac{L_f^{2D} - U_p \cdot b_p}{b_f} \quad (1)$$

In Equation 1, L_f^{2D} is the thermal conductance of the entire section (with insulating panel), U_p is the thermal transmittance of the insulation panel, b_p is the internal side exposed length of the insulation panel, and b_f is the internal side projected length of the frame section. Frame A is shown in Figure 8, where the glazing is replaced with an insulation panel. In both the simulations and experiments, the insulation panel was projecting 15 mm into the frames. That is, the distance is 15 mm from the highest point of the frame on the indoor side, excluding the glazing gasket, to the bottom of the insulation panel. At the same time the insulation panel was projecting 190 mm outwards from the same point.

All frames were drawn using computer-aided design (CAD) files as underlay. Some minor differences may therefore be found between the geometries in the two simulation programs, as different simplifications may be necessary to make a file that may be simulated in the two programs. Double precision was used in both programs.

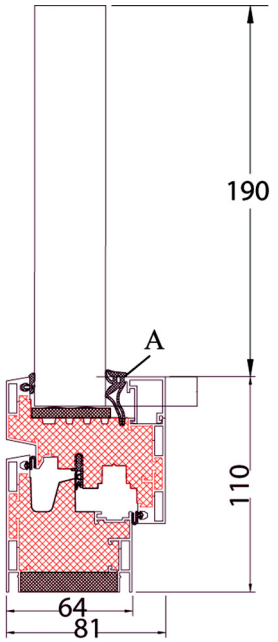

Figure 8 *Cross section of Frame A with insulation panel used instead of a real glazing. The units in the figure are mm.*

Material Properties and Boundary Conditions

Table 3 displays the material properties used in the numerical simulations. Data is from the frame manufacturers when reported. When manufacturers' data was not supplied, material data from ISO 10077-2 (ISO 2003a) was used. The emissivity of all untreated aluminum surfaces was set to 0.2. An emissivity of 0.9 was used for painted surfaces, and 0.8 for anodized surfaces.

The thermal conductivity of the thermal break material (polyurethane) of Frame A was not reported by the manufacturer. However, a density of 400 kg/m^3 was specified for this material. As shown in Table 3, several conductivities are published for such a material. In the simulations we used three different values: 0.03 W/(m·K) (a low value in the reported range), 0.089 W/(m·K) (considered to be a more appropriate value, based on a linear interpolation of conductivities for polyurethane materials with greater and lesser densities than the reported 400 kg/m^3), and 0.121 W/(m·K). When frame and window U-factors are reported, a conductivity of 0.089 W/(m·K) is used unless otherwise stated. The frame U_f-factor reported by the manufacturer was based on measurement, so the conductivity uncertainties should not have any influence on their reported U-factors. In later studies one should consider measuring the conductivity of this material to make sure that the input data is correct.

Table 3. Conductivity and Emissivity of the Materials Used in the Frame Section

Material	Frame	Density, kg/m^3	Emissivity[2]	Thermal Conductivity, W/(m·K)
Aluminum	A		0.2/0.9[5]	160
Ethylene propylene diene monomer (EPDM) (all gaskets)	A		0.9	0.25
Polyurethan-Hartschaum ("EP 2718-5", Rohdichte)	A	400[1]	0.9	0.03[3,4]/0.089/0.121
Steel, oxidized (hardware)	A		0.8	50
Extruded polystyrene	A	33[1]	0.9	0.029
Acrylic (gasket between frame and glazing)	B		0.9	0.2
Aluminum, anodized	B		0.8	160
EPDM (gasket between the solid parts of the frame)	B		0.9	0.25
Fiberglass	B		0.9	0.231
Polyurethane	B		0.9	0.029
Steel, oxidized (hardware)	B		0,8	50
Wood	B		0.9	0.12
Aluminum	C, D		0.2	160
EPDM (gasket between frame and glazing)	C, D		0.9	0.25
Nordic pine	C, D		0.9	0.12
Polyurethane 120M	C, D		0.9	0.029
Schlegel QLon (gasket between the solid parts of the frame)	C, D		0.9	0.03
Basotec (frame cavity filler)	E		0.9	0.035
EPDM (all gaskets)	E		0.9	0.25
PVC	E		0.9	0.17
Steel, oxidized (hardware)	E		0.8	50
Insulation panel	A-E		0.9	0.035

1. As noted by the manufacturer.
2. Estimated values; not stated in the documentation or reported by the manufacturer.
3. From Wärmedämmstoffe (2009): Thermal conductivity = 0.020–0.030 W/(m·K).
4. ISO 10077-2 (ISO 2003a) notes that the design thermal conductivity of rigid polyurethane should be 0.25 (density equal to 1200 kg/m^3).
5. Emissivity of 0.9 is used for painted exposed surfaces, while 0.2 is used for untreated (internal) surfaces.

The air properties used in the CFD simulations were evaluated at the mean temperature of indoor and outdoor air (10°C) and at an atmospheric pressure of 101,325 Pa (see Table 4). The standard acceleration of gravity, 9.8 m/s^2, was used in all calculations. For the hot box experiments the mean temperature was also 10ºC.

Simplified ISO 10077-2 (ISO 2003a) boundary conditions, shown in Table 5, were used in the CFD simulations. The surface heat transfer coefficients combine for a total surface heat transfer resistance of 0.17 (m^2·K)/W, which is the same value used in the hot box experiments (see the Experimental Procedure section of this paper). In the FEM simulations, two types of boundary conditions were used—a fixed coefficient as in the CFD simulation and a more sophisticated model (based on the NFRC 100 [NFRC 2001] boundary conditions) as prescribed by Mitchell et al. (2006). The exterior side boundary condition uses a fixed convection coefficient. In addition, the radiation portion of the surface heat transfer is calculated for each segment, as if it views only a blackbody enclosure of the exterior temperature. The interior side boundary condition also evaluates the radiation exchange for each surface segment separate from a fixed convection coefficient, using a more sophisticated view factor radiation model that includes the effects of self-viewing surfaces of the frame and foam glazing panel. These NFRC-style radiation boundary conditions (used with 0°C and 20°C outside/inside temperatures) were used when comparing FEM simulations to hot box results, while the simplified CEN coefficients were used when comparing CFD to FEM results.

RESULTS

This section presents the experimental and numerical results. Table 6 displays the whole-window U_w-factors and the centre-of-glazing U-factors from the hot box measurements (original glazing installed). The centre-of-glazing U-factor is based on measurements with a 1 mm thick heat flow meter and

Table 4. Air Properties Used in the CFD Simulations

$(T_{in} + T_{out})/2$, °C	λ, $W \cdot m^{-1} \cdot K^{-1}$	c_p, $J \cdot kg^{-1} \cdot K^{-1}$	μ, $kg \cdot m^{-1} \cdot s^{-1}$	ρ, $kg \cdot m^{-3}$	β, K^{-1}
10.0	0.02482	1005.5	1.7724×10^{-5}	1.2467	3.5317×10^{-3}

Table 5. Boundary Conditions Used in the Simulations

Description	Temperature, *T*, °C (K)	Heat Transfer Coefficient, *h* $W/(m^2 \cdot K)$
CFD and FEM simulations (ISO 2003a)		
Inside boundary condition	20.0 (293.15)	7.692
Outside boundary condition	0.0 (273.15)	25.0
FEM simulations (NFRC radiation)		
Frame inside boundary condition	20	2.44 + radiation, with self-viewing
Frame outside boundary condition	0	26 + radiation, with no self-viewing

Table 6. Whole-Window U_w-Factors from the Hot Box Measurements and the Centre-of-Glazing U-Factor Based on Measurements with a 1 mm thick Heat Flow Meter

Frame	$U_{w;\ with\ glazing,\ hot\ box}$, $W/(m^2 \cdot K)$	$U_{central\text{-}glazing,\ hot\ box}$, $W/(m^2 \cdot K)$
A	1.20	0.89
B	0.78	0.74
C	0.84	0.66
D	1.3	1.25
E	n.a.	n.a.

is not equal to the centre-of-glazing U-factor found from calculations according to standards like ISO 15099 (ISO 2003b). The reason for this is that the natural convection correlations used in such standards also include the additional heat loss taking place close to the bottom and top of the glazing cavity. The metering area of the heat flow meter is 50 mm. This U-factor is still useful for obtaining information about the glazing itself. Frame E was not measured with a glazing.

Table 7 shows the U_w-factors from the hot box experiments where an insulation panel is installed in the frame. Frame D was only measured with a glazing. Table 7 also shows the U_w-factors from the CFD and FEM simulations where an insulation panel was installed in the frames. The FEM numerical results are calculated in the simulation program THERM and WINDOW (Mitchell et al. 2006).

Figure 9 shows the window U_w-factor plotted as a function of the thermal break conductivity for Frame A. Conductivities of 0.3, 0.089, and 1.121 W/m·K are used. The results are discussed further in the following section.

Table 8 displays the U_f-factors for the individual frame members (sill, jamb, and head) from CFD and FEM simulations and the difference between these results. In both codes, fixed surface coefficients and the same material properties were used. The main difference is that the CFD code simulates fluid flow inside the air cavities and uses advanced ray-tracing techniques to calculate thermal radiation, while the FEM tool uses simplified correlations for radiation and convection. In the FEM simulations, the air cavities are treated according to NFRC rules and ISO 15099 (ISO 2003b).

DISCUSSION

Windows with Glazing Unit—Hot Box Results

From Table 6 it can be seen that frames B and C have the lowest overall thermal transmittance ($U_{w;\ with\ glazing,\ hot\ box}$), which is below 0.84 $W/(m^2 \cdot K)$, with a three-layer glazing. These frames are made of wood with polyurethane as a thermal break in the sill, head, and jambs. These values can be anticipated from the data supplied by the manufacturers. Both frames are supposed to satisfy the passive house requirements of windows with a U_w-factor less than 0.8 $W/(m^2 \cdot K)$ (Passiv 2010). Discrepancies may be because of window size (the passive house requirement applies for window sizes of 1.23 × 1.48 m, while the tested samples in this work were about 1.2 × 1.2 m) and glazing uncertainties (gas concentration and glass coating uncertainties). With a triple glazing, the glazing will (usually) have a lower U-factor than the frame, and thus as the total window size increases the window U_w-factor will decrease.

The aluminum window frame A, however, has a higher U-factor than expected. This window should also comply with the passive house requirements (Passiv 2010). The reason for this rather high value is probably due to a puncture of the glazing during transport, leading to the heavy gas (Krypton) having leaked out, or to the glazing not having the anticipated specifications (low-e coatings). This shows that it is important to treat the glazing with care and that it is important that the glazing matches the required specifications.

The wood frame D, which is partially insulated (sill does not have a polyurethane break), has a thermal transmittance of 1.3 $W/(m^2 \cdot K)$ with a double-layer glazing. This is outside the

Table 7. Whole-Window U_w-Factors from Hot Box Measurements and CFD and FEM Simulations, Where the Glazing Has Been Replaced with an Insulation Panel

Frame	$U_{w;\ with\ insul.\ panel,\ hot\ box}$, W/(m²·K)	$U_{w;\ with\ insul.\ panel,\ CFD}$, W/(m²·K)	$U_{w;\ with\ insul.\ panel,\ FEM}$, W/(m²·K)
A	0.99	0.992	1.036
B	0.68	0.698	0.723
C	0.70	0.727	0.749
D	n.a.	1.166	1.171
E	0.75	0.811	0.829

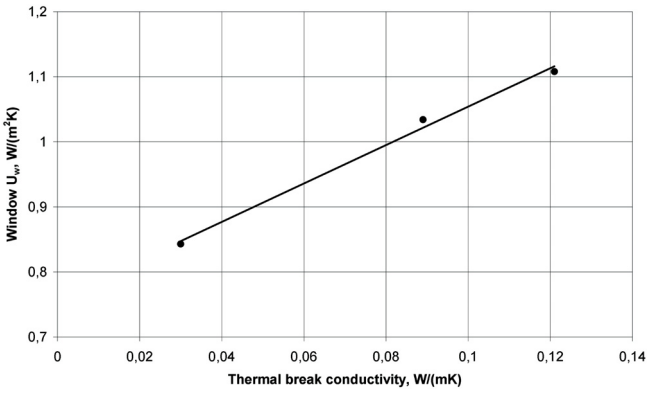

Figure 9 *Whole-window U_w-factor (with insulation panel) versus the thermal break conductivity for Frame A.*

range specified by the manufacturer (U_w-factor between 0.9 and 1.2 W/(m²·K)).

Frame E was not measured with a glazing.

Windows with Insulation Panel— Hot Box and Numerical Results

Table 7 shows the results for the frames with an insulation panel installed. Hot box, CFD, and FEM results are presented. Here the uncertainty of the glazing's thermal performance has been removed since the glazing has been replaced with an expanded polystyrene panel (with a thermal conductivity measured in a hot plate apparatus). By looking at the hot box experiments, it can be seen that the wood frame specimens (B and C) have the lowest thermal transmittance (U_w-factor around 0.7 W/(m²·K)) while the PVC frame (E) has a slightly higher thermal transmittance (U_w-factor around 0.75 W/(m²·K)). The aluminum frame (A) has a U_w-factor of 0.99 W/(m²·K). This relative performance is only true for this series of five windows and no trend of material type versus performance can be expected based on this data; design as well as material choice is important in ultimate performance. By comparing the hot box and numerical U_w results, it can be seen that most of the numerical results from both the FEM and CFD programs are higher than the experimental results. Further, the CFD results compare better with the hot box results than the FEM results. Note that a direct comparison between the FEM and CFD results cannot be done because different boundary conditions are used in these U_w simulations. However, the same boundary conditions are used for the U_f results, which are compared in the following section, and the impacts of slightly different boundary conditions with high-performance products is minimal. The reason for the difference in numerical and experimental results may be due to uncertainties in cavity correlations (radiation and/or convection) in the numer-

Table 8. Window Frame U_f-Factors from FEM and CFD Models; Results for Windows with Insulation Panel Only

Frame*	$U_{f,\ CFD}$, W/(m²·K)	$U_{f,\ FEM}$, W/(m²·K)	% Difference
A sill 1	0.820	0.870	6.1
A jamb 1	0.811	0.900	11.0
A head 1	0.811	0.839	3.5
A sill 2	1.401	1.412	0.8
A jamb 2	1.385	1.494	7.9
A head 2	1.393	1.395	0.1
B sill	0.676	0.746	10.4
B jamb	0.704	0.870	23.6
B head	0.684	0.751	9.8
C sill	0.836	0.874	4.5
C jamb	0.802	0.925	15.3
C head	0.768	0.831	8.2
D sill	1.344	1.394	3.7
D jamb	1.105	1.192	7.9
D head	1.076	1.116	3.7
E sill	0.768	0.812	5.7
E jamb	0.752	0.865	15.0
E head	0.761	0.812	6.7

* Two thermal break material conductivities were simulated for Frame A: 0.03 W/(m·K) (denoted "1") and 0.089 W/m·K (denoted "2").

ical simulations or in the boundary conditions; the results are discussed further in the following section to examine this in more detail.

Figure 9 shows the effect of using various thermal conductivities for the thermal break material of Frame A. And as seen from the figure, changing the conductivity from 0.03 to 0.121 W/(m·K) results in a change in the window U_w-factor from about 0.85 to about 1.1 W/(m^2·K)). This shows the importance of using the correct material properties when calculating the thermal performance, and also the potential for improving the frame thermal performance by using materials with a lower conductivity.

CFD and FEM U_f-Factor Comparison

In Table 8 the CFD and FEM U_f-factors are compared for the individual frame members (sill, jambs, and head). The main differences between the two models in these simulations are the cavity modeling. The CFD code has previously been proven to produce good results (Gustavsen et al. 2001).

For all simulations it is noted that the FEM tool produces U-factors that are slightly higher than those in the CFD code. It can further be seen that the difference between the FEM and CFD codes seems to be lowest for window frames with the highest U-factors (Frames D and A, where the thermal break is simulated with a higher conductivity of 0.089 W/(m·K)). This indicates that the inaccuracies in the frame modeling get more important as the frame U_f-factor decreases. And since the thermal conduction is quite straightforward to model, it is probable that the inaccuracies are a result of the correlations used for the frame cavities.

Another interesting observation can be seen for all the jamb results. The CFD results indicate that the U-factor should be lower for jamb frame members than for the other frame members (if the frame cross sections are otherwise identical). This is consistent with the expectation that thermal convection effects are slightly smaller for vertical frame cavities (jambs) than for horizontal frame cavities (heads and sills). The thermal radiation effects, on the other hand, should be quite similar, if the cross section of the cavities looks about the same. In particular, Frames A and E clearly demonstrate this effect, because the equal cross sections for sills, heads, and jambs are only distinguished by cavity orientation. In contrast, the FEM results indicate higher U-factors for jamb orientations, and the largest discrepancies between CFD and FEM results are the jambs.

To explain the difference in results between the CFD and FEM codes based on ISO 15099 (ISO 2003b), the radiation and natural convection correlations of ISO 15099 need to be examined in more detail. For frame cavities, the effective conductivity, which accounts for both radiative and convective heat transfer, should be calculated according to

$$\lambda_{eff} = (h_{cv} \times h_r) \times d \,, \qquad (2)$$

where λ_{eff} is the effective conductivity, h_{cv} is the convective heat transfer coefficient (found from Nusselt number correlations), h_r is the radiative heat transfer coefficient, and d is the thickness or width of the air cavity in the direction of heat flow. The radiative heat transfer coefficient h_r is the following:

$$h_r = \frac{4\sigma T_{av}^3}{\frac{1}{\varepsilon_{cc}} + \frac{1}{\varepsilon_{ch}} - 2 + \frac{1}{\frac{1}{2}\left\{\left[1 + \left(\frac{L_h}{L_v}\right)^2\right]^{1/2} - \frac{L_h}{L_v} + 1\right\}}} \qquad (3)$$

This equation is developed for a two-dimensional rectangular cavity having height L_v and length L_h where the heat flow direction is in the horizontal direction. The average temperature T_{av} is equal to $(T_{cc} + T_{ch})/2$, where T_{cc} is the temperature of the cold side and T_{ch} is the temperature of the hot (warm) side of the cavity. The symbols ε_{cc} and ε_{ch} are the emissivities of the cold and hot (warm) sides of the cavity, respectively. If the heat flow direction is vertical, then the inverse of the ratio L_h/L_v shall be used.

The radiative heat transfer coefficient h_r is plotted as a function of the vertical aspect ratio L_h/L_v in Figure 10 and, as expected, the radiative heat flow coefficient increases as a function of the vertical aspect ratio L_h/L_v. But since Equation 3 is developed for two-dimensional flow, this will be valid for cavities where the width W of the cavities is very large compared to the length L_h separating the hot and the cold walls. For the three-dimensional cavities typically found in jamb sections of window frames (see Figure 11), the width W of the cavities will be of the same order as the length L_h separating the hot and cold walls. Thus, for jambs the ratio L_h/W should be used to calculate the radiative coefficient instead of L_h/L_v. This illustrates the need for ISO 15099 (ISO 2003b) to be updated to correctly use W instead of L_v for jambs. The authors of the FEM tool are aware of this issue and are in the process of addressing this discrepancy in their software tool.

The natural convection correlations in ISO 15099 (ISO 2003b) are also a result of studies of cavities where the width W of the cavities are much higher than the length L_h. This will also result in higher heat transfer rates for jamb sections when

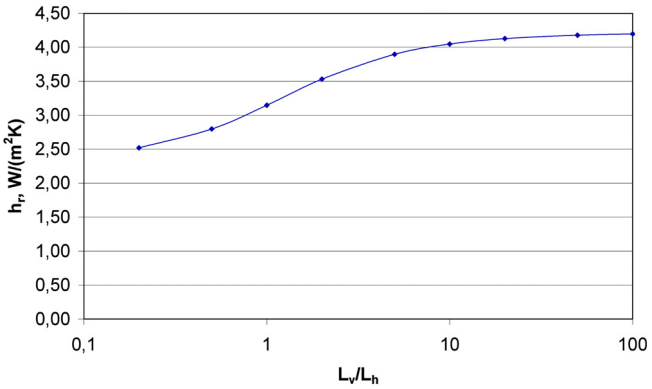

Figure 10 *The radiative heat transfer coefficient as a function of* L_v/L_h *for a two-dimensional cavity.*

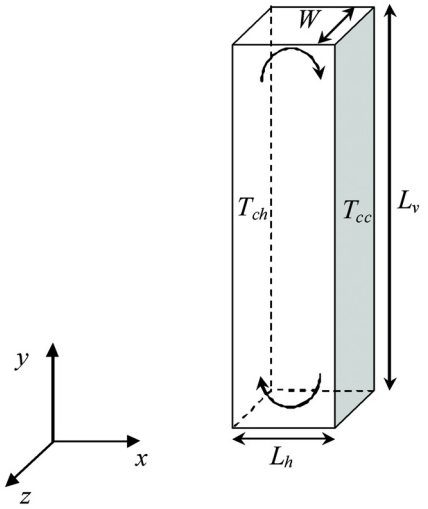

Figure 11 *Three-dimensional representation of a frame cavity. To find the heat transfer correlations used in ISO 15099 (ISO 2003b), the length* L_h *is assumed to separate two isothermal walls. For both the convection and radiation correlations in ISO 15099,* W *is assumed to be much higher than* L_h.

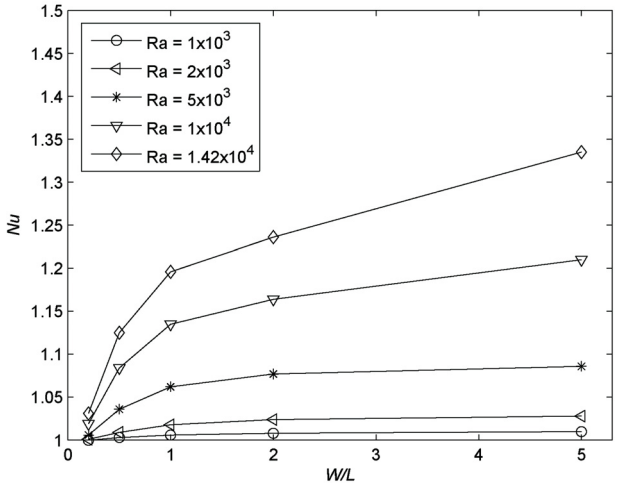

Figure 12 *Average Nusselt number plotted as a function of the Rayleigh number (Ra) and for different horizontal aspect ratios,* W/L_h. *The vertical aspect ratio,* L_v/L_h, *is equal to 40. The symbol* L *is equal to* L_h *in Equation 3 and Figure 11—the length separating the two isothermal walls. The figure is from Gustavsen and Thue (2007).*

the calculations are based on these ISO 15099 correlations compared to three-dimensional CFD simulations where the actual frame cavity is considered. This is also shown in Figure 12, where the Nusselt number is plotted as a function of Rayleigh number and horizontal aspect ratio W/L_h for a cavity where the vertical aspect ratio L_v/L_h is equal to 40 (Gustavsen and Thue 2007). Nusselt number correlations valid for cavities typically found in jambs have been proposed by Fomichev et al. (2007) and Gustavsen and Thue (2007).

CONCLUSIONS AND FURTHER WORK

This paper compares hot box experiments, finite element method calculations (with air cavity treatment according to the window calculation standard ISO 15099 [ISO 2003b]), and computational fluid dynamics simulations of heat transfer in high-performance windows and window frames. The results show that there are quite some differences between the various measurement and simulation techniques but that some of these differences might be explained by uncertainties in the underlying correlations that are used to calculate frame cavity heat transfer. The results indicate that there are larger uncertainties (inaccuracies) for better frames (low U_f-factor) than for poorer frames (higher U_f-factors). Further studies will be performed to investigate these results in more detail.

Specifically, we suggest the following:

- ensuring proper testing of the thermal conductivity of materials, especially for thermally breaks;
- that ISO 15099 should be updated to correctly calculate radiation heat transfer in vertical frame cavities (found in jambs);
- that the natural convection correlations proposed for jamb cavities in ISO 15099 should be changed to correlations taking the three-dimensional nature of the fluid flow in such cavities into account; and
- further work on the impacts of penetrating operating hardware on high-performance frames, as the products chosen all had effective thermal breaks around the hardware.

ACKNOWLEDGMENT

This work was supported by the Assistant Secretary for Energy Efficiency and Renewable Energy, Office of Building Technology, Building Technologies Program of the U.S. Department of Energy under Contract No. DE-AC02-05CH11231 and by the Research Council of Norway within the research project MOT “Modern Wood Window Frames with Surface Treatment”.

REFERENCES

CEN. 2000. EN ISO 12567-1, *Thermal Performance of Windows and Doors—Determination of Thermal Transmittance by Hot Box Method—Part 1: Complete Windows and Doors*. Brussels: European Committee for Standardization

CEN. 2003. EN ISO 12412-2:2003, Thermal Performance of Windows, Doors and Shutters—Determination of Thermal Transmittance by Hot Box Method—Part 2:

Frames. Brussels: European Committee for Standardization

Finlayson, E., R. Mitchell, D. Arasteh, C. Huizenga, and D. Curcija. 1998. THERM 2.0: Program description. A PC program for analyzing the two-dimensional heat transfer through building products. Berkeley, CA: University of California.

Fluent. 2005. *FLUENT 6.2 User's Guide*. Lebanon, NH: Fluent, Inc.

Fluent. 2006a. GAMBIT 2.3.16. Lebanon, NH: Fluent, Inc.

Fluent. 2006b. *FLUENT 6.3 User's Guide*. Lebanon, NH: Fluent, Inc.

Fomichev, A., D.C. Curcija, B. Balagurunathan, and M. Stocki. 2007. Investigation of heat transfer effects of sloped and ventilated internal cavities of framing systems, Final report. Amherst: Center for Energy Efficiency and Renewable Energy, University of Massachusetts.

Gustavsen, A., and J.V. Thue. 2007. Numerical simulation of natural convection in three-dimensional cavities with a high vertical aspect ratio and a low horizontal aspect ratio. *Journal of Building Physics* 30(3):217–40.

Gustavsen A., B.T. Griffith, and D. Arasteh. 2001. Three-dimensional conjugate computational fluid dynamics simulations of internal window frame cavities validated using infrared thermography. *ASHRAE Transactions* 107(2):538–49.

Gustavsen, A., C. Kohler, D. Arasteh, and D. Curcija. 2005. Two-dimensional conduction and CFD simulations of heat transfer in horizontal window frame cavities. *ASHRAE Transactions* 111(1):587–98.

Gustavsen, A., D. Arasteh, B.P. Jelle, C. Curcija, and C. Kohler. 2008. Developing low-conductance window frames: Capabilities and limitations of current window heat transfer design tools—State-of-the-art review. *Journal of Building Physics* 32(2):131–53.

ISO. 2003a. *ISO 10077-2, Thermal Performance of Windows, Doors and Shutters—Calculation of Thermal Transmittance—Part 2: Numerical Method for Frames*. Geneva: International Organization for Standardization.

ISO. 2003b. *ISO 15099, Thermal Performance of Windows, Doors and Shading Devices—Detailed Calculations*. Geneva: International Organization for Standardization.

Leonard, B.P. 1979. A stable and accurate convective modelling procedure based on quadratic upstream interpolation. *Computer Methods in Applied Mechanics and Engineering* 19(1):59–98.

Mitchell, R., C. Kohler, D. Arasteh, J. Carmody, C. Huizenga, and D. Curcija. 2006. *THERM 5.2/WINDOW 5.2 NFRC Simulation Manual*. Berkeley, CA: Lawrence Berkeley National Laboratory.

NFRC. 2001. *NFRC 100:2001, Procedure for Determining Fenestration Product U-factors*. Silver Spring, MD: National Fenestration Rating Council.

Passiv. 2010. Passivhaus Institute Web site www.passiv.de. Germany.

Patankar, S.V. 1980. *Numerical Heat Trasfer and Fluid Flow.* Washington, DC: Hemisphere.

Van Doormaal, J.P., and G.D. Raithby. 1984. Enhancement of the SIMPLE method for predicting incompressible fluid flows. *Num. Heat Transfer* 7:147–63.

Wärmedämmstoffe. 2009. Polyurethan-Hartschaum (PUR). www.waermedaemmstoffe.com/htm/pur.htm.

Yao, J., and W. Fan. 1994. Theory and numerical study on three dimensional discrete transfer radiation model. *Journal of Thermal Science* 3(4):263-66.

Zhao, Y. 1998. Investigation of heat transfer performance in fenestration system based on finite element methods. PhD dissertation, Department of Mechanical and Industrial Engineering, University of Massachusetts, Amherst.